AD-A185 474 AN ANALYSIS OF SIMPLIFIED FEED ARCHITECTURES FOR MMIC (MONOLITHIC MICROWA (U) ROME AIR DEVELOPMENT CENTER GRIFFISS AFB NY J L POIRIER FEB 87 1/1

UNCLASSIFIED F/G 17/9 NL

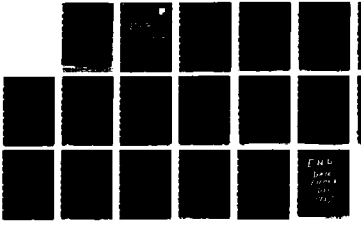

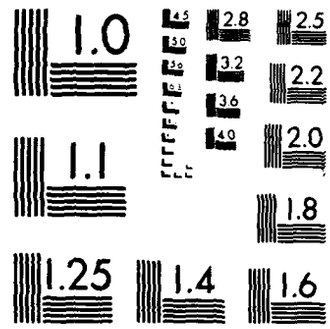

MICROCOPY RESOLUTION TEST CHART
NATIONAL BUREAU OF STANDARDS-1963-A

DTIC FILE COPY

(12)

AD-A185 474

RADC-TR-86-236
In-House Report
February 1987

AN ANALYSIS OF SIMPLIFIED FEED ARCHITECTURES FOR MMIC T/R MODULE ARRAYS

J. Leon Poirier

DTIC
ELECTE
OCT 2 2 1987
S D
H

APPROVED FOR PUBLIC RELEASE; DISTRIBUTION UNLIMITED

ROME AIR DEVELOPMENT CENTER
Air Force Systems Command
Griffiss Air Force Base, NY 13441-5700

87 10 21 003

This report has been reviewed by the RADC Public Affairs Office (PA) and is releasable to the National Technical Information Service (NTIS). At NTIS it will be releasable to the general public, including foreign nations.

RADC-TR-86-236 has been reviewed and is approved for publication.

APPROVED: John K Schindler

JOHN K. SCHINDLER
Chief, Antennas and Components Division
Directorate of Electromagnetics

APPROVED: Allan C Schell

ALLAN C. SCHELL
Director of Electromagnetics

FOR THE COMMANDER: John A. Ritz

JOHN A. RITZ
Directorate of Plans & Programs

If your address has changed or if you wish to be removed from the RADC mailing list, or if the addressee is no longer employed by your organization, please notify RADC (EEC) Hanscom AFB MA 01731-5000. This will assist us in maintaining a current mailing list.

Do not return copies of this report unless contractual obligations or notices on a specific document requires that it be returned.

Unclassified
SECURITY CLASSIFICATION OF THIS PAGE

AD-A185 709

REPORT DOCUMENTATION PAGE

1a. REPORT SECURITY CLASSIFICATION: Unclassified	1b. RESTRICTIVE MARKINGS
2a. SECURITY CLASSIFICATION AUTHORITY	3. DISTRIBUTION / AVAILABILITY OF REPORT: Approved for public release; Distribution unlimited.
2b. DECLASSIFICATION / DOWNGRADING SCHEDULE	
4. PERFORMING ORGANIZATION REPORT NUMBER(S): RADC-TR-86-236	5. MONITORING ORGANIZATION REPORT NUMBER(S)
6a. NAME OF PERFORMING ORGANIZATION: Rome Air Development Center; 6b. OFFICE SYMBOL (If applicable): EEC	7a. NAME OF MONITORING ORGANIZATION
6c. ADDRESS (City, State, and ZIP Code): Hanscom AFB, Massachusetts 01731	7b. ADDRESS (City, State, and ZIP Code)
8a. NAME OF FUNDING / SPONSORING ORGANIZATION: Rome Air Development Center; 8b. OFFICE SYMBOL (If applicable): EEC	9. PROCUREMENT INSTRUMENT IDENTIFICATION NUMBER
8c. ADDRESS (City, State, and ZIP Code): Hanscom AFB, Massachusetts 01731	10. SOURCE OF FUNDING NUMBERS: PROGRAM ELEMENT NO 62702F; PROJECT NO 4600; TASK NO 15; WORK UNIT ACCESSION NO 07

11. TITLE (Include Security Classification)
An Analysis of Simplified Feed Architectures for MMIC T/R Module Arrays

12. PERSONAL AUTHOR(S)
J. Leon Poirier

13a. TYPE OF REPORT	13b. TIME COVERED	14. DATE OF REPORT (Year, Month, Day)	15. PAGE COUNT
In-House	FROM Jun 86 TO Oct 86	1987 February	30

16. SUPPLEMENTARY NOTATION

17. COSATI CODES			18. SUBJECT TERMS (Continue on reverse if necessary and identify by block number)
FIELD	GROUP	SUB-GROUP	Active aperture phased array Transmit receive module Noise in phased arrays
	1709		
	2014	2003	

19. ABSTRACT (Continue on reverse if necessary and identify by block number)

MMIC T/R modules offer the possibility for simplifying the feed networks of active aperture phased arrays. In particular, the addition of amplitude control along with the existing phase control would allow the same feed network to be used in the transmit and receive modes even though the two require grossly different aperture tapers. This is easily accomplished by using the amplitude control in the modules to provide the weighting required to produce low sidelobe receive beams.

Specific examples in which amplitude control is implemented with digital attenuators are examined. The effect of the attenuators on the array output signal-to-noise ratio and the error sidelobe level due to the amplitude quantization are evaluated. The results indicate that the component values needed—total attenuation 20 to 30 dB, low noise amplifier gains and noise figures 20 to 30 dB and 3 to 4 dB respectively, and quantization of 2 to 6 bits—are readily achievable in current GaAs technology. With these, active -

(Contd)

20. DISTRIBUTION / AVAILABILITY OF ABSTRACT	21. ABSTRACT SECURITY CLASSIFICATION
☒ UNCLASSIFIED/UNLIMITED ☒ SAME AS RPT ☐ DTIC USERS	Unclassified
22a. NAME OF RESPONSIBLE INDIVIDUAL: J. Leon Poirier	22b. TELEPHONE (Include Area Code): (617) 377-2526 — 22c. OFFICE SYMBOL: RADC/EEC

DD FORM 1473, 84 MAR — 83 APR edition may be used until exhausted. All other editions are obsolete.

SECURITY CLASSIFICATION OF THIS PAGE
Unclassified

19. (Contd)

aperture monopulse arrays with sidelobe levels of -20 to -50 dB below the peak of the mainbeam may be designed with greatly simplified feed networks.

Preface

I would like to thank John Antonucci and Edward Staffier for their indispensable help. Mr. Antonucci developed the programs for calculating the Taylor and Bayliss array element weights and also the array patterns. Mr. Staffier operated the computer and produced all the computer generated figures in this report.

Thanks also, to Philipp Blacksmith, Daniel Jacavanco, and Dr. Peter Franchi for reading the manuscript and offering their suggestions for its improvement.

Accession For
NTIS GRA&I ☑
DTIC TAB ☐
Unannounced ☐
Justification
By
Distribution/
Availability Codes
Dist | Avail and/or Special
A-1

Contents

Illustrations

Illustrations

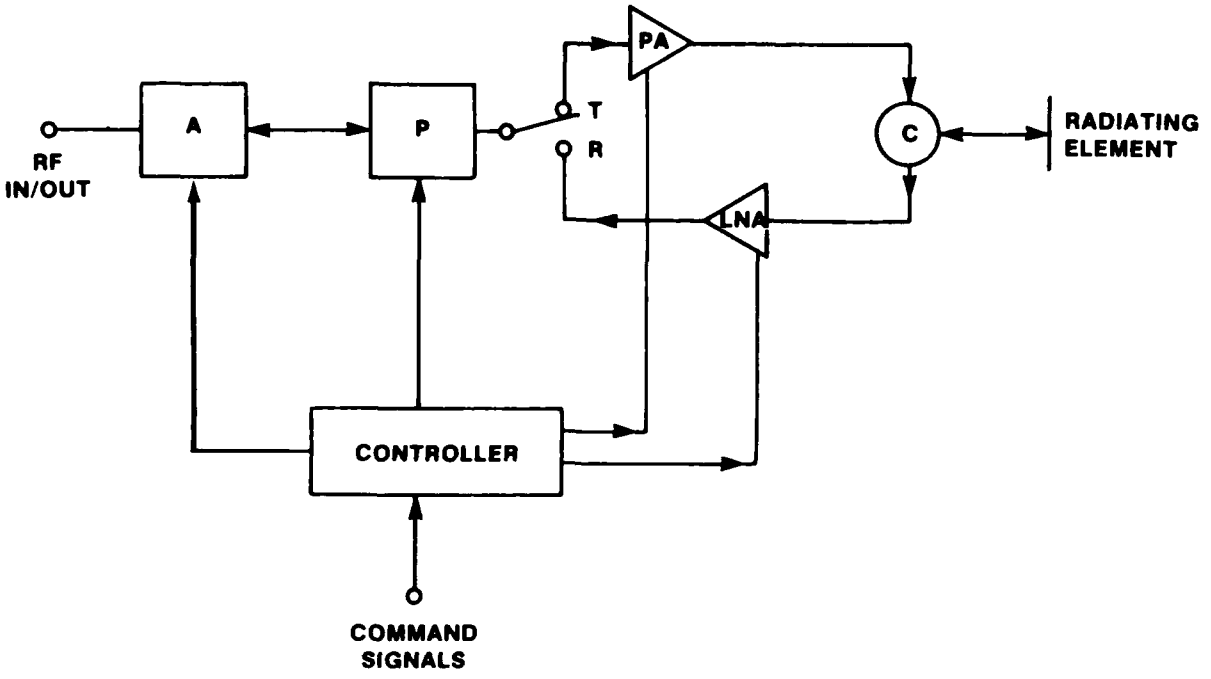

Figure 1. Typical MMIC Transmit/Receive Module

It appears likely that amplitude control represented by variable attenuator A will be provided in at least some module designs. This would allow control of the output power in order to impose modest tapers on the transmit aperture distribution, provide a better match among channels to control the error sidelobe level, and enable the aperture distribution to be modified as a function of scan angle in conformal antennas. In the latter case, aperture control in the curvature plane is necessary to prevent spreading of the grating lobes into visible space and to preserve the depth of the monopulse notch as the beam is scanned off boresight.

A column of an antenna system of a low sidelobe monopulse radar array antenna is shown in Figure 2a. The system uses a module at each element and three feed networks to produce a transmit, a low sidelobe sum, and a low sidelobe difference beam. The column outputs are further combined in appropriately weighted azimuth beamformers. Here, the transmit beam feed network is assumed to be uniformly weighted to achieve maximum efficiency but any other taper could also be applied. The sum and difference receive beamformers are weighted with tapers such as the Taylor and Bayliss respectively to produce the low sidelobe levels required to reduce the system's vulnerability to interference from clutter or other sources.

Notice that the common input/output port on the module must be duplexed with an external switch or circulator to connect it to the appropriate beamformer on

An Analysis of Simplified Feed Architectures for MMIC T/R Module Arrays

1. INTRODUCTION

Monolithic Microwave Integrated Circuit (MMIC) transmit/receive modules make possible new phased array antenna architectures. This report examines the possible simplification of the feed networks of a monopulse radar array when the flexibility of an MMIC module is fully utilized. In particular, using the module's internal amplitude control will allow a single beamformer to be shared between the transmit and receive modes even though the amplitude taper for each mode is dramatically different.

The circuit arrangement of a typical MMIC module is shown in Figure 1. It is made up of a power amplifier PA, a low noise amplifier LNA, a phaser P, a variable attenuator A, a controller, and a system that selects between the transmit and receive mode. In the transmit mode, the T/R switches provide a connection from the input of the module through the phaser, the PA, and the circulator to the antenna. The T/R system also includes receiver protection in this mode. On receive, the signal path is through the LNA and the PA turned off to conserve power. In both modes, the phaser is set to the appropriate phase, selected by the controller in response to a command, to produce a beam in the desired direction.

(Received for publication 26 February 1987)

transmit and receive. Also, a power divider is needed in each channel to split the received signal between the two beamformers. The specific form of beamformer network depends on the design of the array, but stripline dividers will probably be used in MMIC application. The upper and lower halves of the array are combined to produce the three beams in the vertical plane.

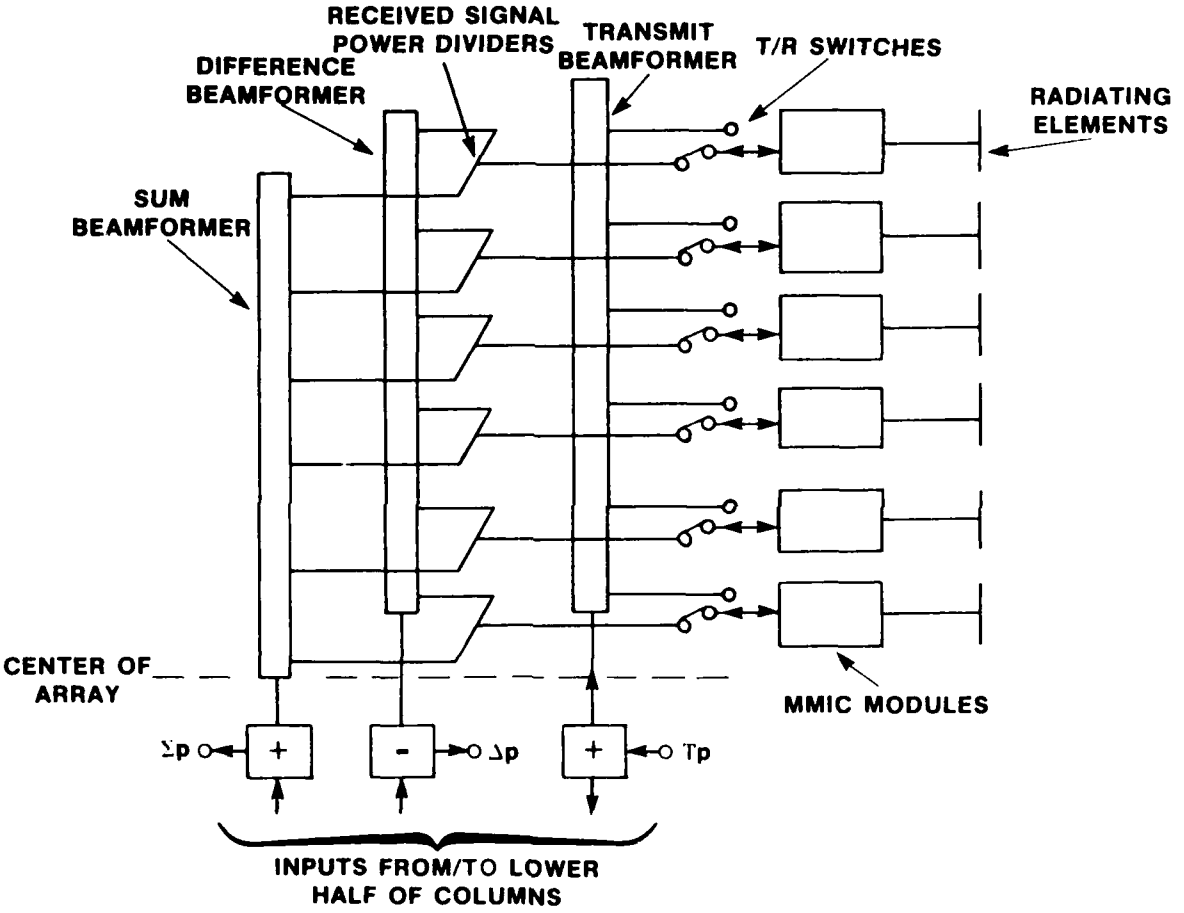

Figure 2a. Vertical Antenna Networks for Monopulse Radar (Conventional Arrangement)

When each module has amplitude control, the arrangement shown in Figure 2a can be greatly simplified. Instead of using the amplitude control only for channel matching and scan correction for conformal arrays, it can also be used to generate the illumination function for one of the receive beams. In this way, one beamformer can be shared between the transmit and receive modes thereby eliminating one of the receive beam feed networks.

Figure 2b shows an antenna system in which the module and antenna have been closely integrated. Here only two beamformers are needed instead of three. One of these is uniformly tapered and the other is specially modified to produce a low sidelobe difference pattern from the signals that have been corrected to produce a low sidelobe sum beam. The former is used for both transmit and receive. In the transmit mode, it operates exactly as before and delivers a co-phased, equal amplitude signal to each module's common input/output terminal. On receive, however, the module amplitude control is activated and adjusts the amplitude of each module's received signal before feeding into the beamformer to produce a low sidelobe Taylor or similarly weighted sum beam at the network's output.

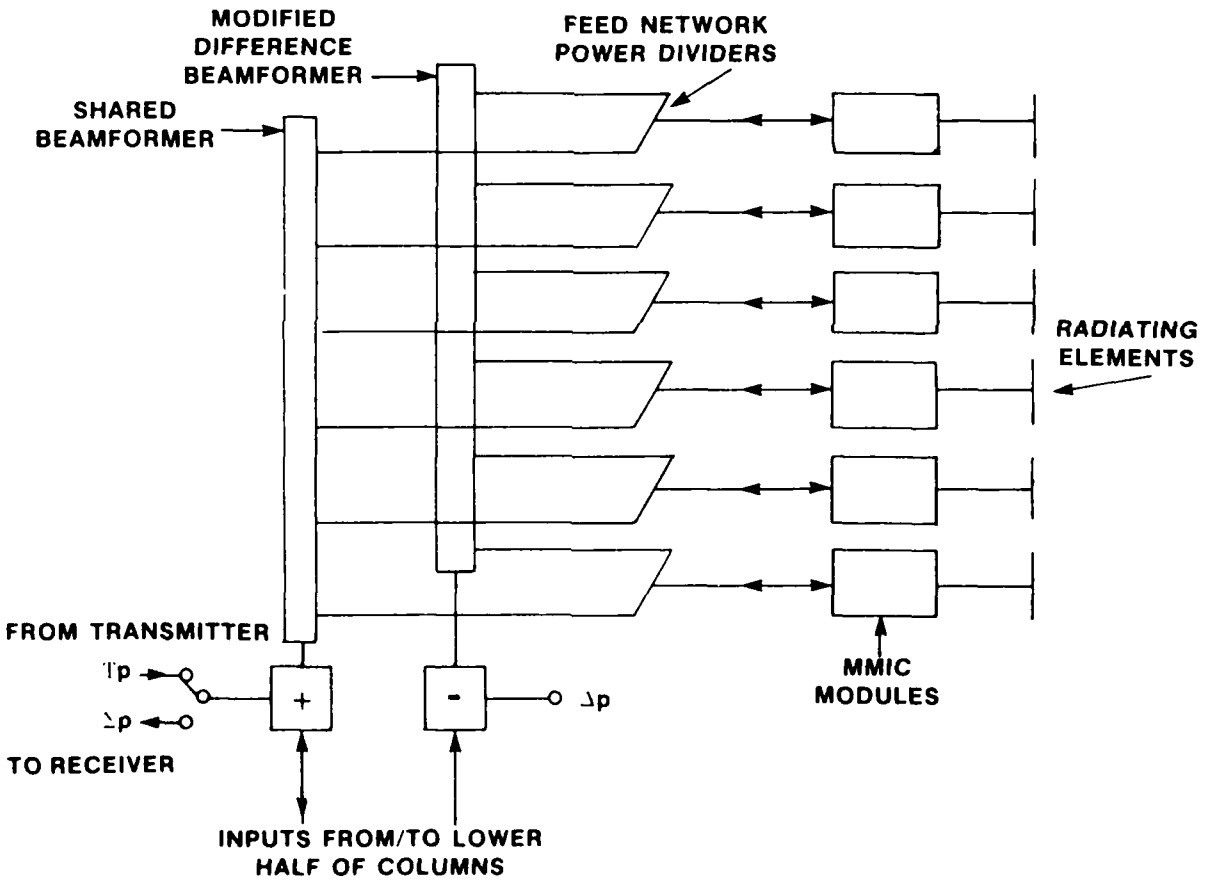

Figure 2b. Vertical Antenna Networks for Monopulse Radar (Shared Beamformer Arrangement)

On receive, the amplitudes of the module output signals are varied along the column to produce the tapering for the low sidelobe sum beam and incidently the signals for the difference beam. Thus the difference beam feed network must be specially weighted to accommodate these input signals to produce ultimately the required difference weighting function at the Δ channel output.

It now remains to investigate the practicability, limitations, and impact on module design of incorporating the idea of a shared beamformer into an antenna system.

2. SYSTEM CONSIDERATION

2.1 Aperture Weighting

The element signals, after passing through the LNA are appropriately attenuated and appear at the module output with a low sidelobe taper distribution. When these outputs are combined in the uniform beamformer network, the beamformer output will be the low sidelobe Σ pattern. However, the difference channel signals must also be derived from these weighted module output signals. The beamformer weighting necessary to produce a low sidelobe difference pattern is chosen according to the rule

$$k_q \quad k_{\Delta q}/k_{\Sigma q} \tag{1}$$

where k_{Σ} and k_{Δ} are the required sum pattern and difference pattern weight respectively.

An example of the relative weighting for $\bar{n}$ = 4, SLL = -30 dB Taylor Σ and Bayliss Δ patterns for a 64-element linear array are shown in Figure 3. It can be seen that peak values of the two occur at different positions in the aperture. Equation (1) was used to calculate the modified weighting that is needed to convert the Taylor distribution into the similarly characterized Bayliss distribution. The modified Bayliss weighting is represented by the dashed curve in the figure.

2.2 Range of Attenuation

The range of adjustment of the attenuator that is necessary depends on the SLL of the design. In general, the lower the sidelobe level, the greater the range of amplitudes required across the array to produce the taper. The curves in Figure 4 show the range in attenuation required to achieve various sidelobe levels for

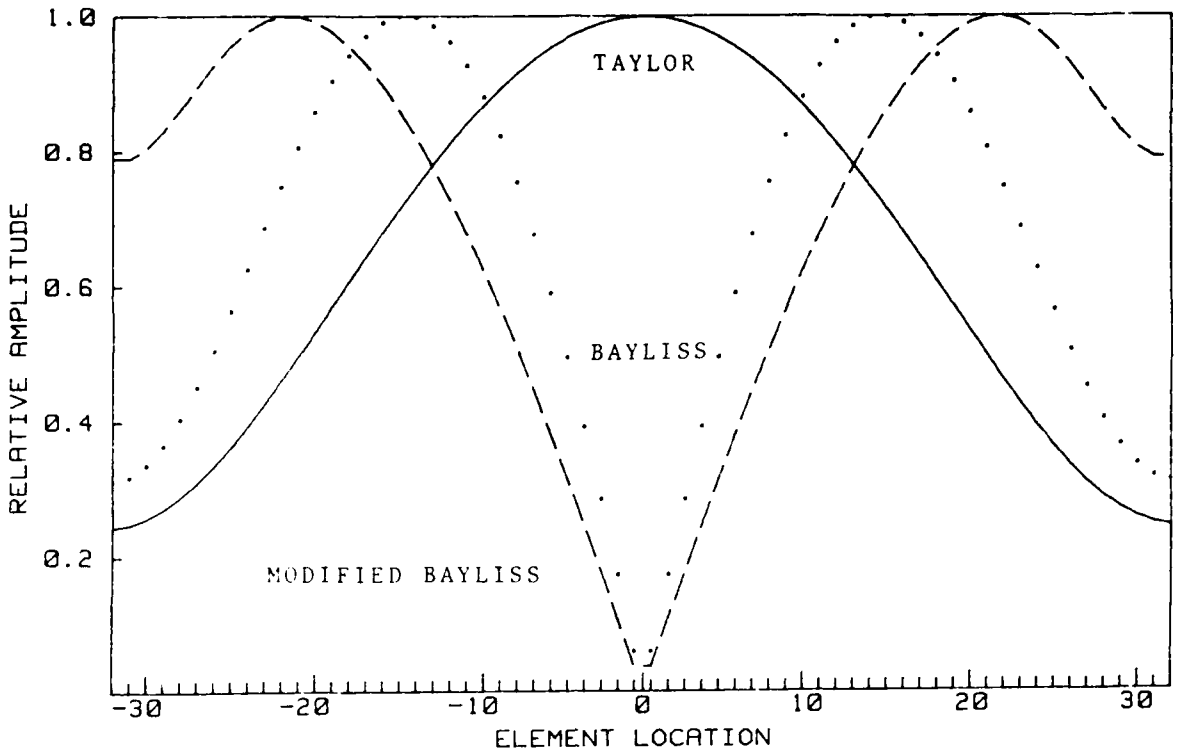

Figure 3. Comparison of Element Weights for Taylor, Bayliss, and Modified Bayliss Distributions. $\bar{n}$ = 4, SLL = -30 dB, and Q = 64

several $\bar{n}$ values for Taylor weighting.[1,2,3] For example, an $\bar{n}$ = 6, SLL = -40 dB design requires a maximum taper attenuation of about 19.4 dB relative to the center element. Thus, if the taper is implemented by attenuators, then the attenuator must have a range of 20 dB (assuming identical modules at every element). It is apparent that the maximum taper weight is not a sensitive function of $\bar{n}$ and the maximum attenuation A of the attenuator may be conveniently approximated by

$$A \approx (11/15)(SLL + 20) - 5 \text{ dB} . \qquad (2)$$

Thus the attenuator value for a Taylor weighted aperture depends only on the side-lobe level of the design. Equation (2) is represented by the dashed line in the figure.

1. Hansen, R.C. (1964) Microwave Scanning Antennas, Volume I, Academic Press, New York.

2. Elliot, R.S. (1981) Antenna Theory and Design, Prentice-Hall, Englewood Cliffs, New Jersey.

3. Barton, D.K., and Ward, H.R. (1969) Handbook of Radar Measurement, Prentice-Hall, Englewood Cliffs, New Jersey.

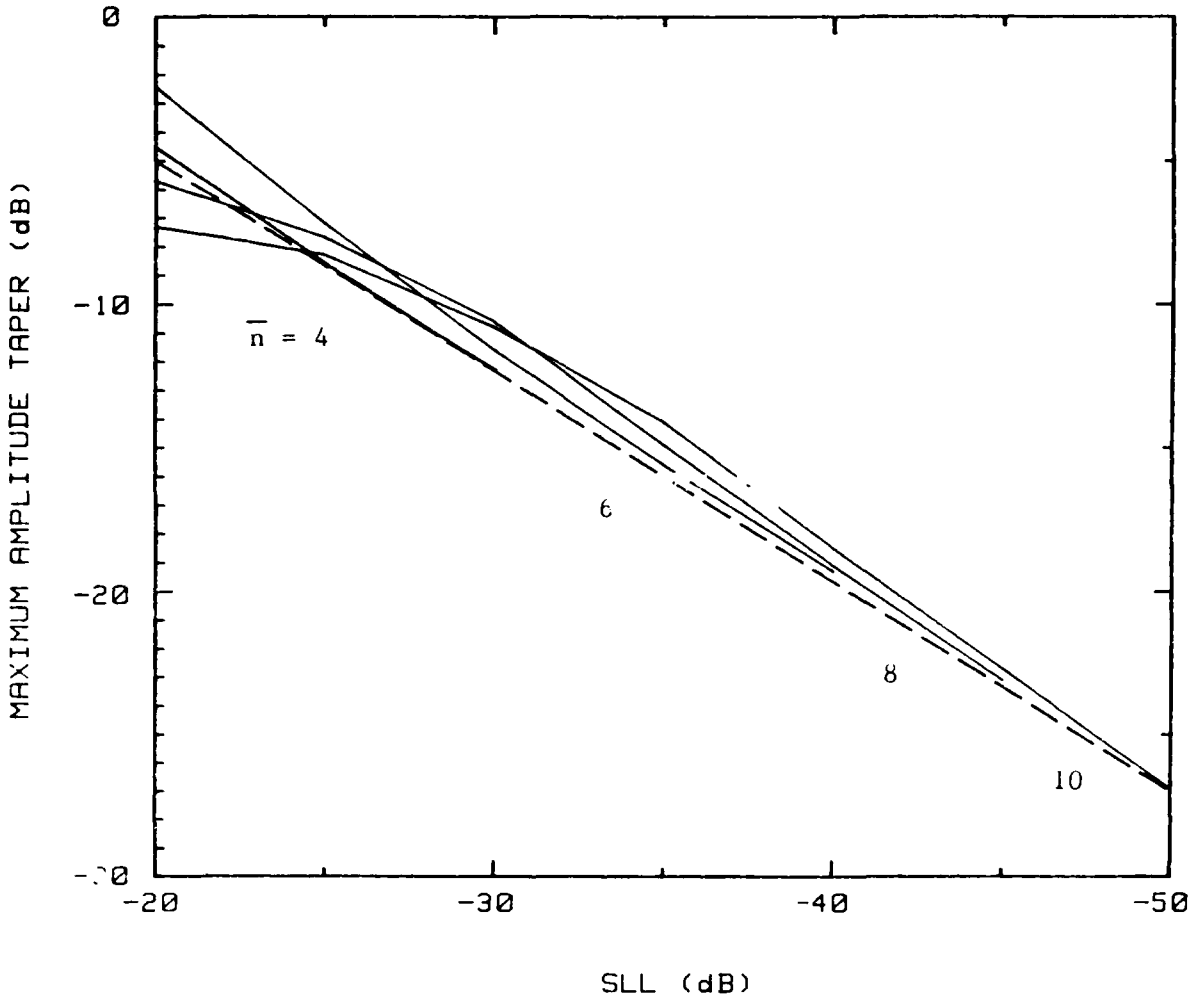

Figure 4. Maximum Element Taper for Linear Taylor Weighted Arrays

2.3 Amplitude Quantization Error

The value of attenuation produced by each module will be quantized. The error sidelobes due to quantization of the element amplitudes must be less than the sidelobe level SLL of the design. The rms error sidelobe level due to phase and amplitude errors can be found from the expression

$$SLL_{rms} \approx (\sigma_P^2 + \sigma_A^2)/(1 - \sigma_P^2)M\eta_t \qquad (3)$$

where σ_P^2 and σ_A^2 are the variances of the total phase and amplitude errors from all sources respectively, M the number of elements, and η_t the aperture

taper efficiency.[4] It should be noted that M and η_t in Eq. (3) apply to the entire aperture. For example, a rectangular aperture of Q rows and P columns would make M = QP and $\eta_t = \eta_{tQ}\eta_{tP}$. The total variances σ_P^2 and σ_A^2 are equal to the sums of the variances from all contributing sources of the phase and amplitude errors respectively. The variance due to a phase shifter quantization of B bits is $\sigma_{Pl}^2 = \pi^2/(3\times 2^{2B})$. For an attenuator of B' bits and total attenuation A (in dB)

$$\sigma_{Al}^2 = 10^{A/10}/(12 \times 2^{2B'}) . \tag{4}$$

Other sources of phase and amplitude errors include mismatch, power division and position errors.

Before the value of the error sidelobe level SLL_{rms} can be found, the taper efficiency η_t must be known. The taper efficiency for a linear array of Q elements is evaluated with the expression

$$\eta_t = \sum_{q=1}^{Q} \sum_{p=1}^{Q} a_q a_p / Q \sum_{q=1}^{Q} a_q^2 \tag{5}$$

where the a_q are the element weights. The results for a linear Taylor weighted array are plotted in Figure 5 for several values of $\bar{n}$. It is apparent that η_t is not a sensitive function of $\bar{n}$ but depends chiefly on SLL. For convenience and later use, η_t for a linear Taylor tapered array is approximated by

$$\eta_t = 0.96 \exp[(SLL + 20)/92.2] . \tag{6}$$

Equation (6) can now be used with Eq. (4) to evaluate the error sidelobe level of Taylor weighted linear arrays for various amplitude quantization levels using Eq. (3). The calculations assume that the only error is that due to the amplitude quantization. The value of A was obtained from Eq. (2). The results are plotted in Figure 6 as a function of SLL. Inspection of the figure shows that for a 64-element array with SLL = -40 dB, a seven-bit quantization of the 20-dB attenuator is needed to achieve an rms error sidelobe level SLL_{rms} = -50 dB. To this would be added the effects of the other sources of error to arrive at the ultimate error sidelobe level from all sources.

4. Haupt, R. L., Capt. (1982) Simultaneous Nulling in the Sum and Difference Patterns of a Monopulse Antenna, RADC-TR-82-274, AD A131865.

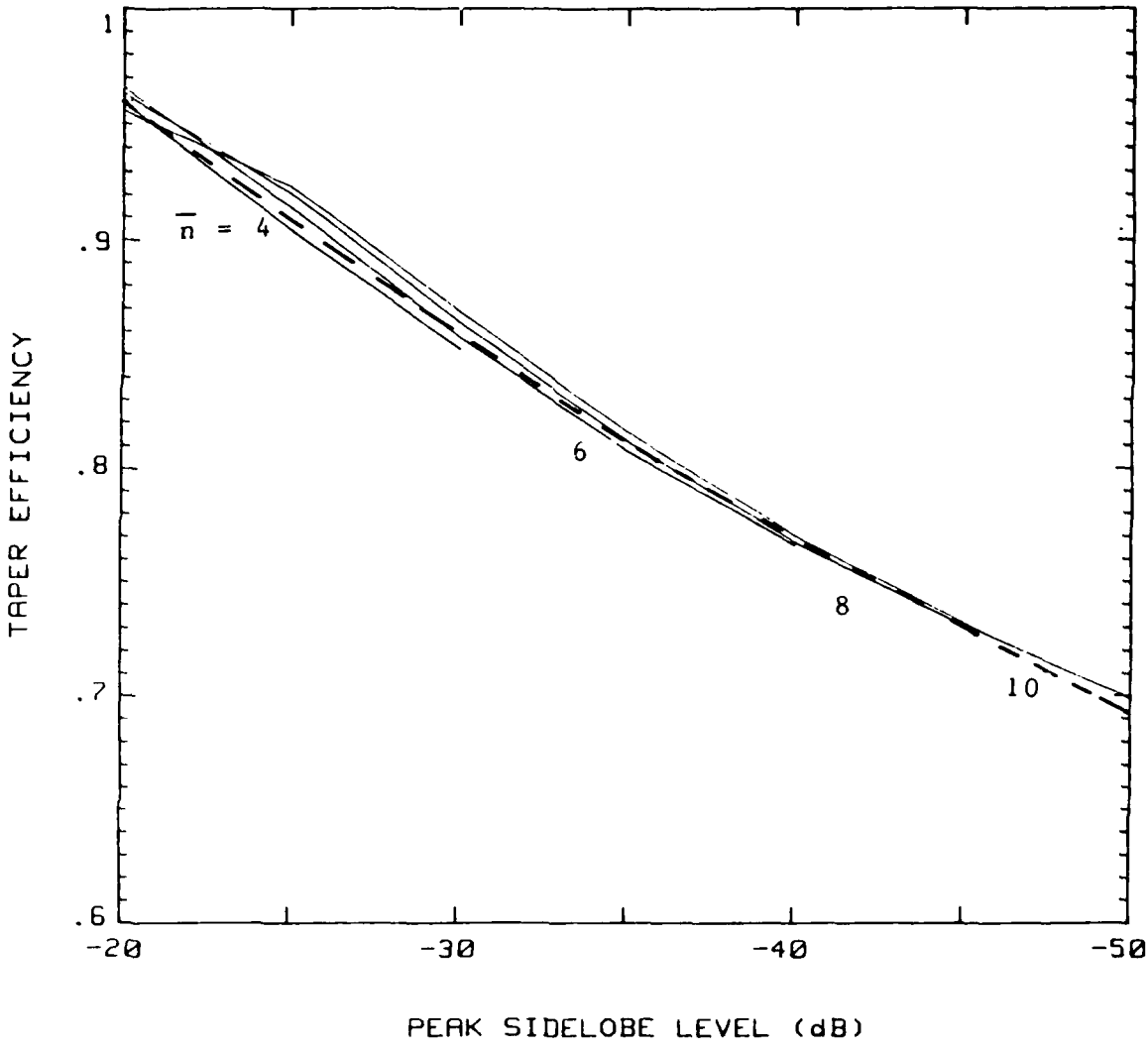

Figure 5. Taper Efficiency for Linear Taylor Weighted Arrays

For a similarly characterized 64 × 64 array, M = QP = 4096. From Eq. (6) $\eta_t = \eta_{tQ}\,\eta_{tP} = 0.60$, and From Eq. (2) A = 20 dB. Here we assume the column outputs are in a conventional Taylor weighted beamformer. Using these values in Eqs. (4) and (3) gives B' ≈ 4.

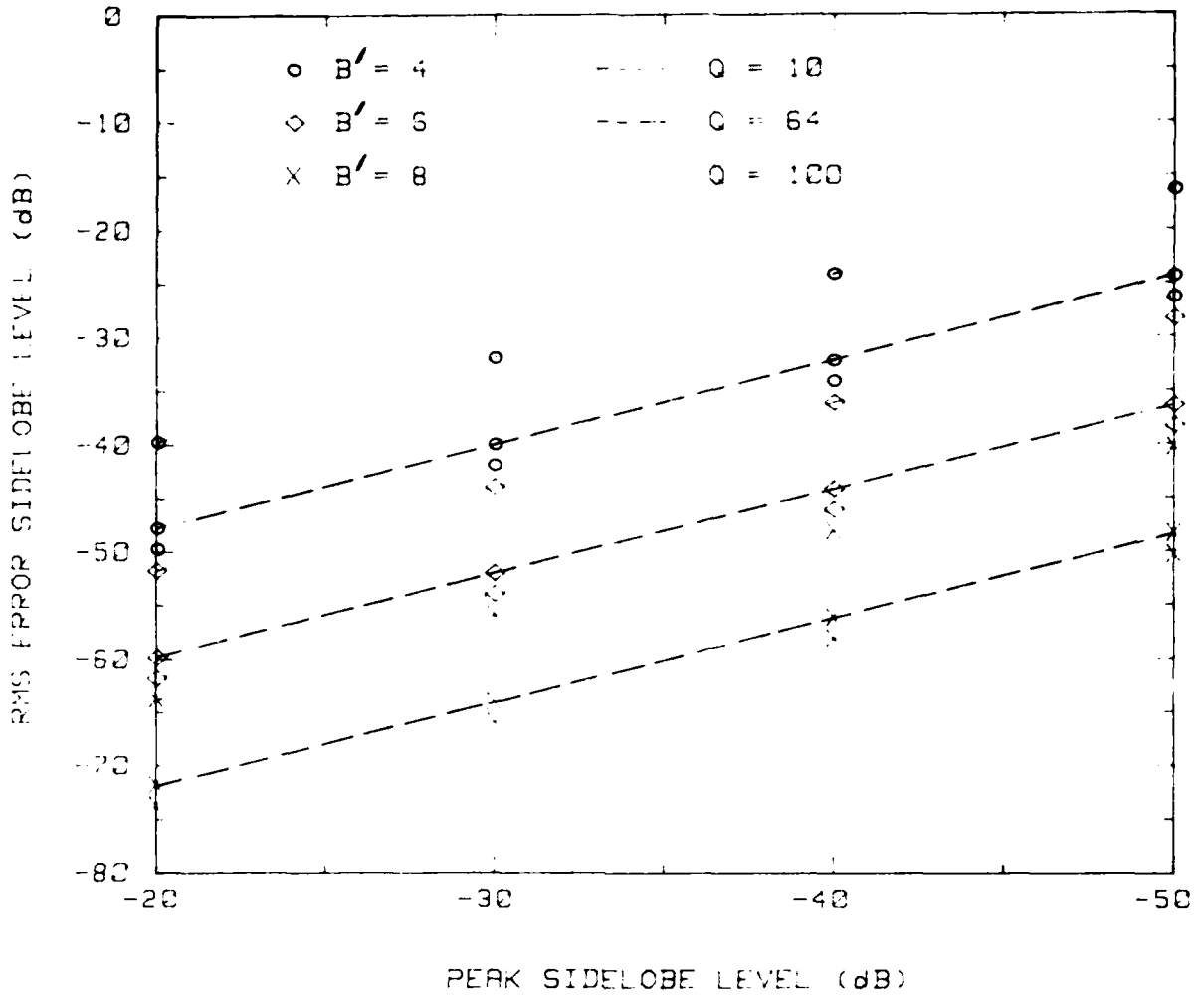

Figure 6. RMS Error Sidelobe Level for Linear Taylor Weighted Arrays. A and η_t were obtained from Eqs. (2) and (6) respectively, as a function of SLL. $\lambda/2$ element spacing

The effect of the attenuator quantization on the antenna patterns is shown in Figure 7. The right half of Figure 7a shows the error-free pattern for a 64-element linear array with $\bar{n}$ = 4 and SLL = -30 dB. The left half of the figure shows degradation in the pattern when the taper setting attenuator is quantized to four bits. Figure 7b, right and left halves, shows the patterns that result for three- and five-bits respectively. The patterns are symmetrical about the main-beam because the aperture taper and the quantization errors as well are symmetrically distributed. It is apparent that the larger the value of B', the smaller the error.

The quantization errors also effect the difference pattern. The modified Bayliss weighting computed from Eq. (1) is error free. However, the Taylor weighted

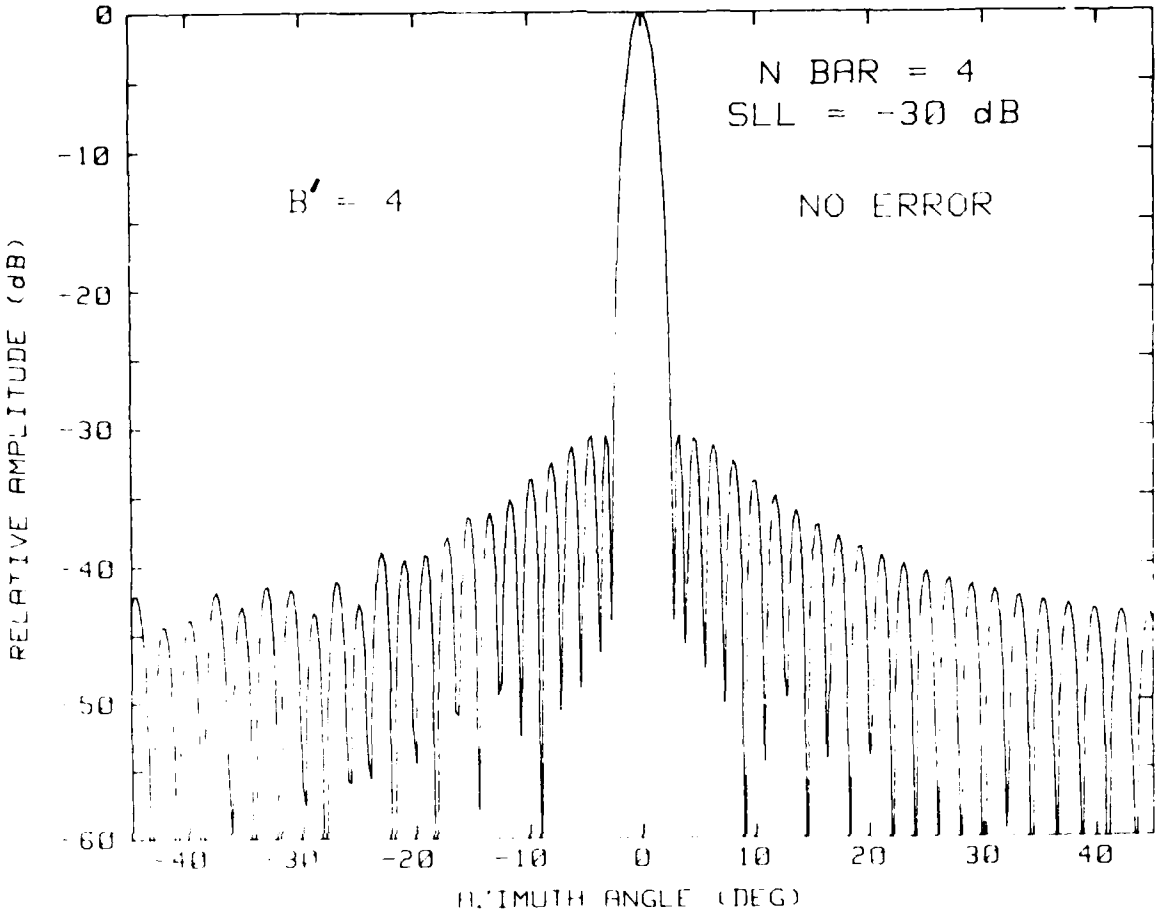

Figure 7a. Effect of Amplitude Quantization on Sum Channel Patterns (Right and Left Halves Show No Error and Four-bit Quantization Respectively. 64-element array with $\lambda/2$ spacing

output signals from the modules are correct only to within the attenuator quantization LSB. Therefore the actual signals presented to the difference channel beamformer are errored. The difference patterns that result from Taylor weighted element signals applied to a modified beamformer are shown in Figure 8. The right and left halves of Figure 8a show the error free and four-bit level patterns respectively. Figure 8b, right and left halves, shows the three- and five-bit patterns respectively. The patterns are symmetrical because of taper and errors are symmetrical about the center of the aperture. Because of this, the depth of the notch is not affected by the quantization.

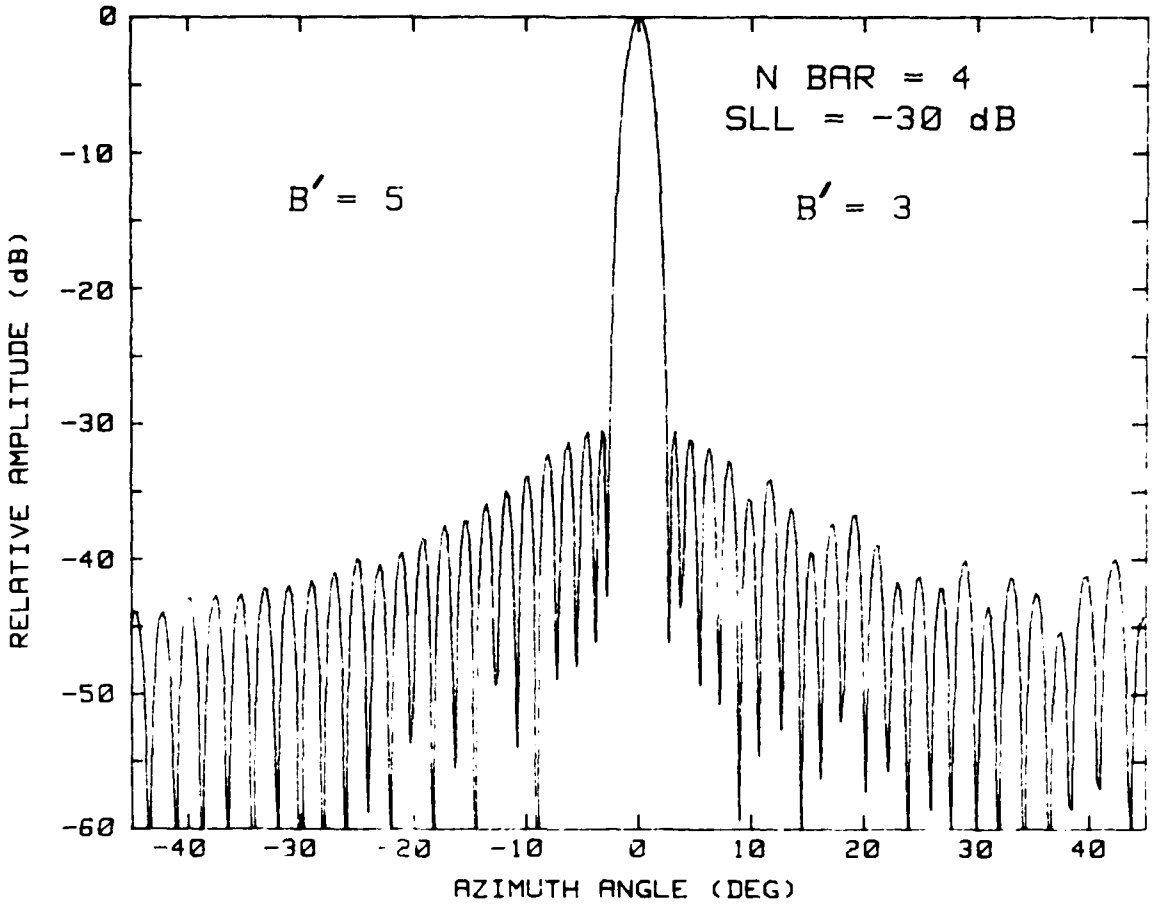

Figure 7b. Effect of Amplitude Quantization on Sum Channel Patterns (Right and Left Halves Show Three- and Five-bit Quantization Respectively). 64-element array with $\lambda/2$ spacing

It should also be noted that the gains of the patterns are somewhat lower than expected. Figure 3 shows that the peaks of the Taylor and Bayliss distributions occur at different aperture locations. Because of this, the Taylor weights must be reduced by a factor of about 0.72 during the application of the modified Bayliss weights that results in an additional loss in gain of about 3 dB in the difference pattern. This additional loss can be eliminated by providing a separate attenuator for the Δ channel. In this case, the power division for the two sum channels would occur ahead of the attenuators so that the output weighting could be independently controlled.

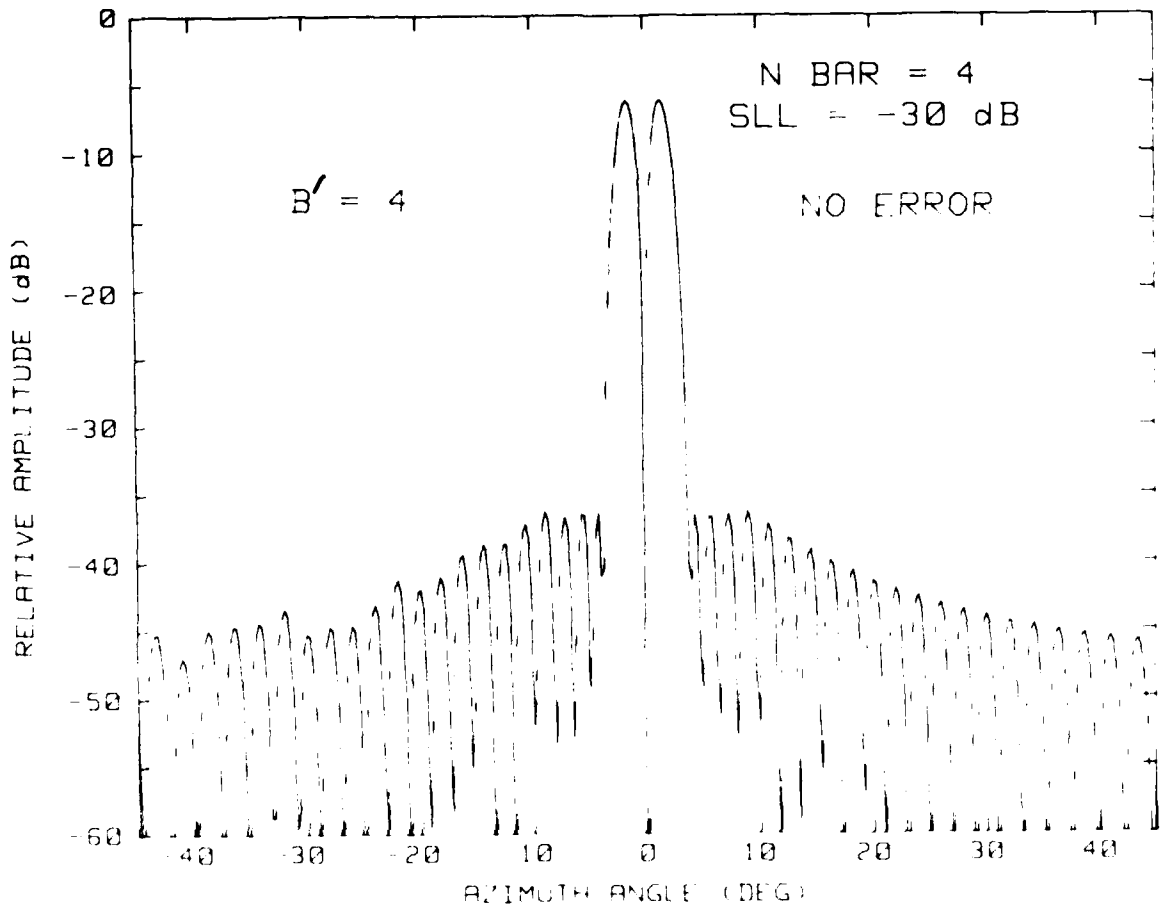

Figure 8a. Effect of Amplitude Quantization on Difference Channel Patterns (Right and Left Halves Show No Error and Four-bit Quantization Respectively). 64-element array with $\lambda/2$ spacing

2.4 Signal-to-Noise Ratio

A sketch of a generalized active array is shown in Figure 9. Each channel contains a low noise amplifier LNA, a digital phase shifter P, and a digital attenuator A. All other circuit channel losses including the insertion losses of the phase shifter, the attenuator, and the beamformer are lumped into L. The signal power at the output of the array may be found by first summing the complex voltage contributions v_q from each element to obtain the output V as

$$V = \sum_{q=1}^{Q} v_q g_q q_q k_q l_q \exp[j\theta_q] \tag{7}$$

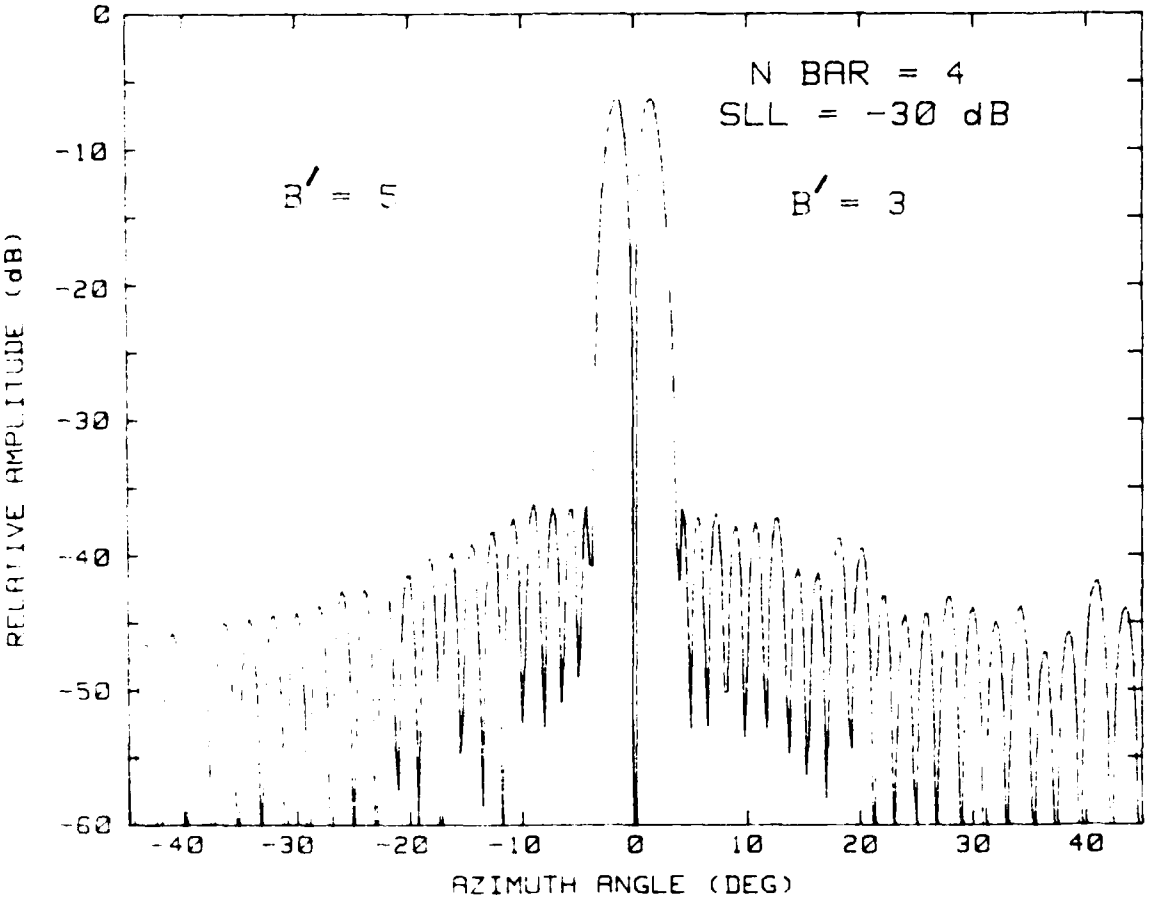

Figure 8b. Effect of Amplitude Quantization on Difference Channel Patterns (Right and Left Halves Show Three- and Five-bit Quantization Respectively), 64 element array with $\lambda/2$ spacing

where g_q is the voltage gain of the LNA, a_q the voltage attenuation of the attenuator, k_q the beamformer relative voltage coupling coefficient (k_q maximum = 1), l_q the fixed voltage attenuation of the channel, and θ_q the total phase shift (including that of the phaser) of the channel. The output power S may be found from

$$S = \sum_{q=1}^{Q} \sum_{p=1}^{Q} v_q v_p g_q g_p^* a_q a_p k_q k_p^* l_q l_p^* \exp[j(\theta_q - \theta_p)] \quad . \tag{8}$$

Similar expressions can be written for the noise contributions.[5] However, since the internally generated noise is independent from channel to channel, the

5. Steinberg, B.D. (1976) Principles of Aperture and Array System Design, Wiley, New York.

power for terms where $q \neq p$ is zero. Thus, the noise power N may be expressed directly in terms of the channel noise power input N_q as

$$N = \sum_{q=1}^{Q} N_q G_q A_q L_q [F_q + (1 - A_q L_q)/A_q L_q G_q] K_q \qquad (9)$$

where $G_q = g_q g_q^*$ and F_q are the power gain and noise figure of amplifier q respectively. The noise figure of the attenuation channel is set equal to the reciprocal of its attenuation[6] and $K_q = k_q k_q^*$ is the power coupling coefficient of the beamformer

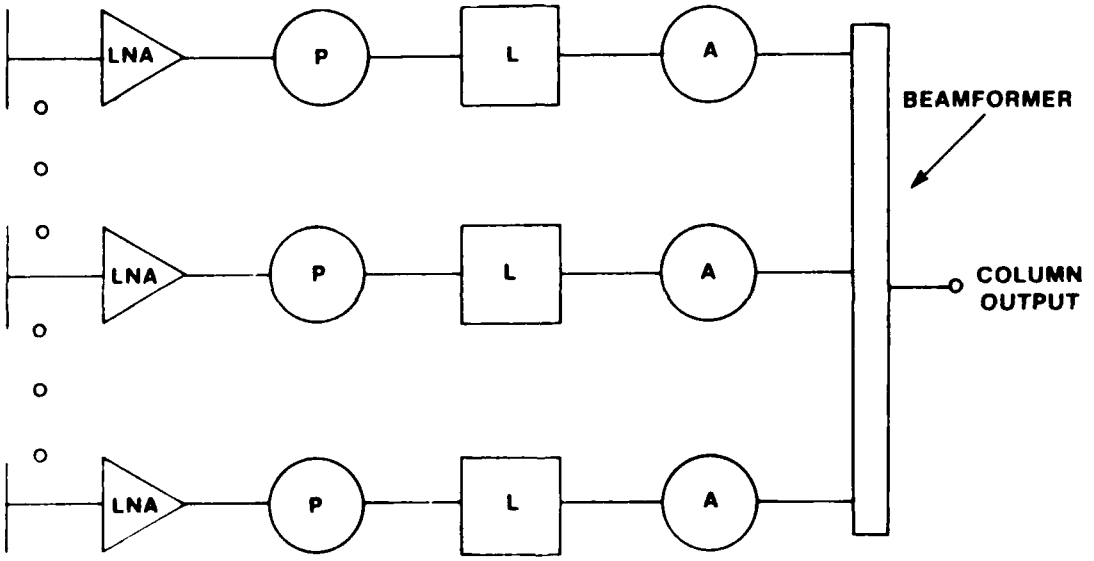

Figure 9. Sketch of Active Aperture Array

Equations (8) and (9) can now be used to find the output S/N ratio of an antenna system in terms of the input S_i/N_i ratio for a wide variety of array configurations. For a lossless array in the mainbeam direction without amplifiers or attenuators and a uniform beamformer, $v_q = v$, $v_q^* = v$, $a_q = 1$, $l_q = 1$, $g_q = 1$, $k_q = 1$, and $vv^* = S_i$ so that

$$S/N = (S_i/N_i)Q \quad . \qquad (10)$$

6. Carlson, B. A. (1975) Communication Systems, 2nd Ed., McGraw-Hill, New York.

Allowing for equal circuit losses $l_q l_p = L < 1$ in each channel results in the expression

$$S/N = (S_i/N_i) LQ \ . \tag{11}$$

The effect of circuit losses L is apparent. To reduce the impact of losses on the S/N ratio, a low noise amplifier may be inserted into the system at each element. Then Eqs. (8) and (9) give

$$S/N = (S_i/N_i) Q/[F + (1 - L)/LG] \ . \tag{12}$$

For a wide range of values, S/N depends principally on the noise figure of the amplifier and thus attenuation in the array components is not as important. In fact for $LG >> 1$,

$$S/N = (S_i/N_i) Q/F \ . \tag{13}$$

For low sidelobe tapered arrays, the improvement in S_i/N_i is not as great as for uniform arrays because the taper efficiency of the array reduces the signal power S. Also, the edge elements, for which attenuation is large compared to the gain of the amplifier, introduce proportionally more noise when the taper is set by attenuators and the beamformer coupling is uniform.

This can best be seen by inserting Eq. (5), the aperture taper efficiency η_t into Eq. (8). Then, an array with a uniform beamformer ($K_q = 1$), the same amplifier in each channel ($G_q = G$ and $F_q = F$), the same total losses in each channel ($L_q = L$), and the aperture weighting determined by attenuators A_q would display a signal-to-noise of

$$S/N = \{(S_i/N_i) Q \eta_t/F\} \sum_{q=1}^{Q} A_q / \sum_{q=1}^{Q} A_q[1 + (1 - A_q L)/A_q LGF] \ . \tag{14}$$

When $A_q LG >> 1$, S/N becomes

$$S/N = (S_i/N_i) Q\eta_t/F \ . \tag{15}$$

Thus Eqs. (14) and (15) for tapered arrays correspond respectively to Eqs. (12) and (13) for uniform arrays.

It is convenient to write Eq. (14) as

$$S/N = (S_i/N_i)Q\eta_t\eta_s/F \tag{16}$$

where the aperture noise suppression efficiency η_s is defined as

$$\eta_s = \sum_{q=1}^{Q} A_q \Big/ \sum_{q=1}^{Q} A_q[1 + (1 - A_qL)/A_qLGF] \ . \tag{17}$$

η_s represents the additional reduction in S/N caused by the noise contributed by the array components. $\eta_s = 1$ for a lossless uniform array without amplifier or attenuators ($A_q = 1$, $G = 1$, $F = 1$, $L = 1$) and $\eta_s = L$ for the same but lossy array ($A_q = 1$, $G = 1$, $F = 1$). The aperture noise suppression efficiency is plotted in Figure 10 for a range of typical values for tapered active arrays. As expected, η_s decreases with SLL (for a fixed value of G) because increasingly larger attenuation is needed to produce the taper. It is apparent, however, that so long as G is sufficiently large compared to A and L the decrease in S/N can be kept small.

2.5 Azimuth Feed Networks

Figure 2a shows the vertical feed network connections. These outputs must now be combined in the azimuth beamformers as shown in Figure 11a. The column index number is p. The weighted sums of the Σp outputs for $p < 0$ and $p > 0$ are also subtracted to produce the low sidelobe azimuth difference beam $\Sigma\delta$. The Δp outputs are similarly divided and combined to produce the elevation difference beam $\Delta\sigma$. The transmit beam $T\sigma$ combining network is uniformly weighted and interconnects all the transmit vertical beamformers. Thus the input to this network is ultimately equally divided among every element in the array. The elevation difference-azimuth difference $\Delta\sigma$ beamformer at the bottom of Figure 11a is used for adaptive nulling arrays and not normally provided as an output.

It is apparent that a fully implemented low sidelobe array requires three elevation beamformers and a mode transfer switch at each of P columns and five azimuth beamformers. Together, these produce a total of five beams. The setup in Figure 11a can be used with the array systems in either Figure 2a or Figure 2b since each has three separate outputs. However, the shared beamformer arrangement can also be applied to the azimuth $T\sigma$ and $\Sigma\sigma$ channels thereby eliminating an azimuth beamformer and P mode transfer switches at the outputs of the vertical beamformers.

This simplified arrangement is sketched in Figure 11b. The uniformly weighted shared beamformer is used for both the transmit beam, and together with

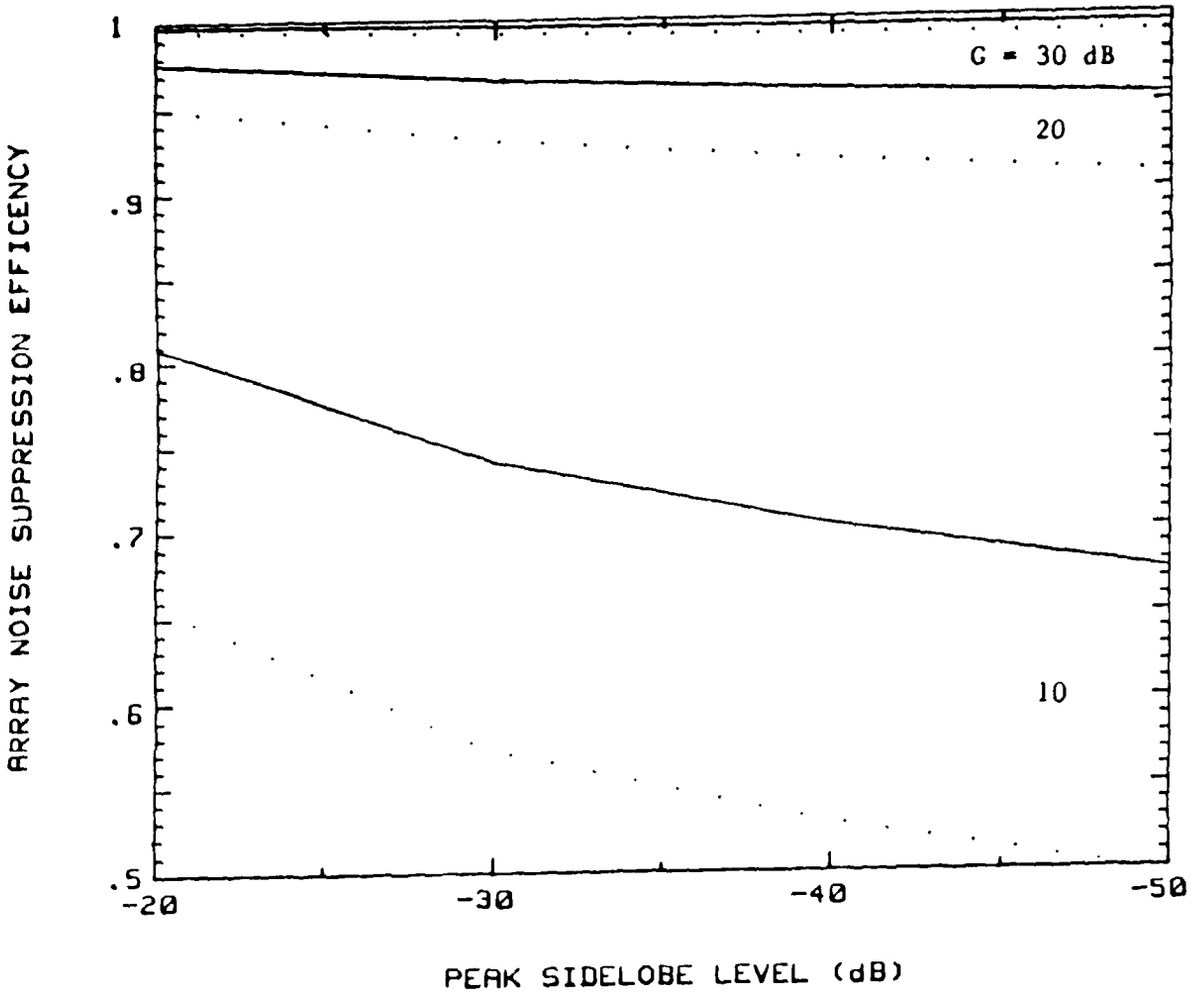

Figure 10. Aperture Noise Suppression Efficiency for Linear Taylor Weighted Arrays. Q = 64, F = 3 dB, and spacing is $\lambda/2$. Solid curves L = -6 dB, dotted curves L = -9 dB

amplitude adjustment in the modules, the $\Sigma\sigma$ receive beam. With this arrangement, the attenuators in the modules are adjusted to form the elevation distribution. Simultaneously, the azimuth weighting is applied by increasing the attenuation in all modules of a column as a function column position. As before, the weighting for the azimuth difference beamformer must be modified because its inputs will have a Taylor or similar weighting.

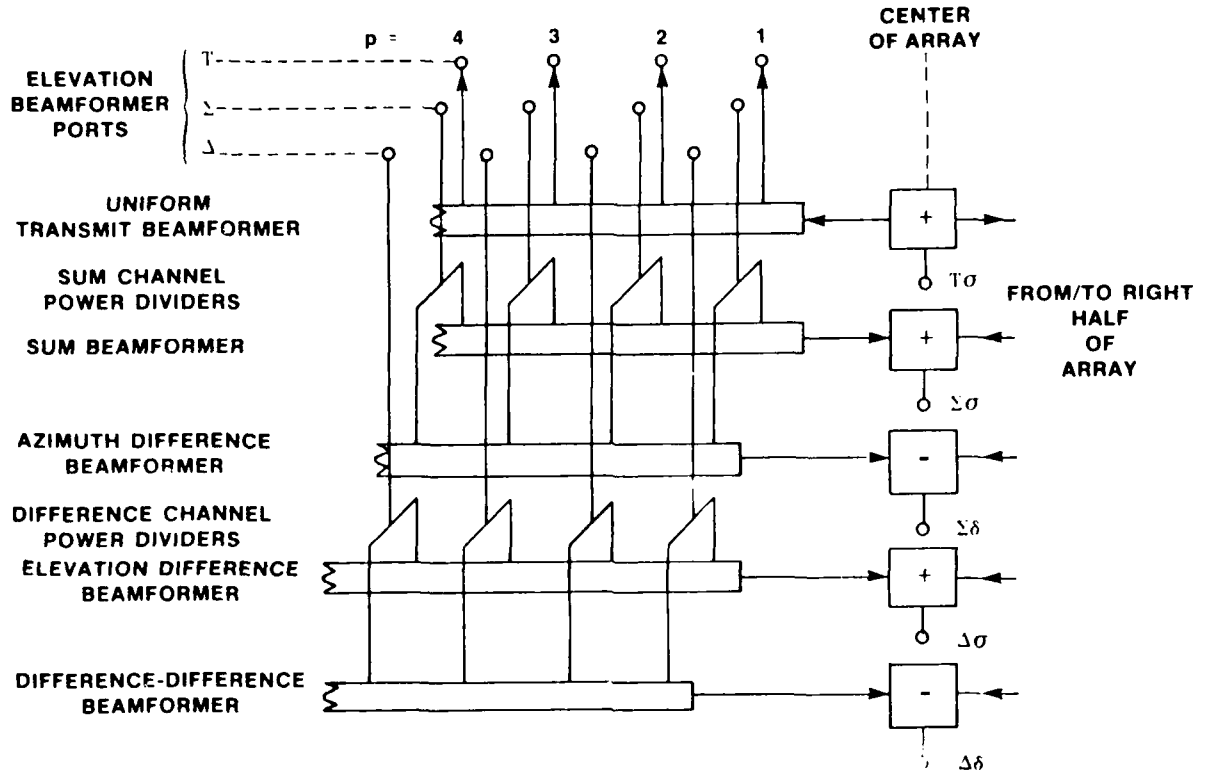

Figure 11a. Antenna System for Monopulse Radar (Conventional Arrangement)

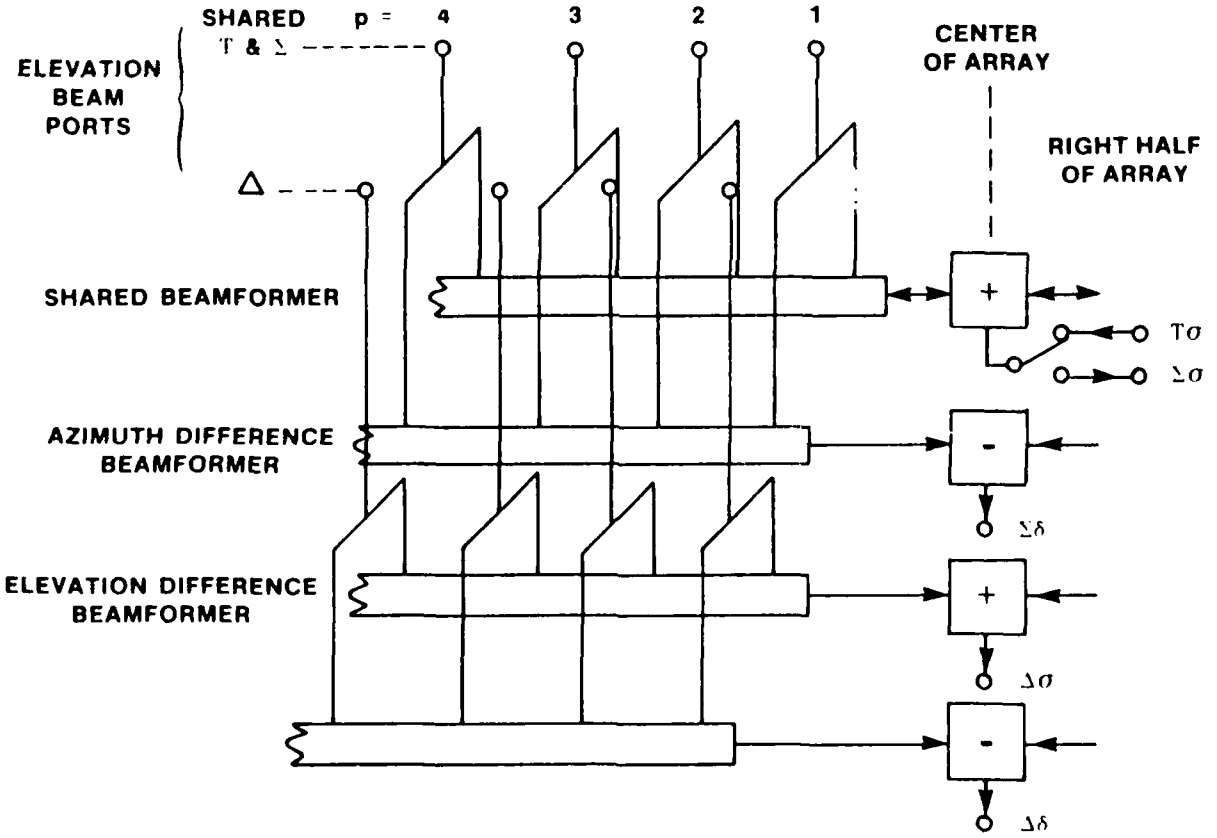

Figure 11b. Antenna System for Monopulse Radar (Shared Beamformer Arrangement)

3. EXAMPLE

As an example, a 64 × 64 array is implemented with the shared beamformer idea. The total number of elements M = PQ = 4096. The goals are SLL = -40 dB and -30 dB below the peak for the azimuth and elevation planes respectively.

First, the maximum taper required was obtained from Figure 4 or Eq. (2). This determines the value of A. However, in a rectangular array the azimuth and elevation weights, if both set by the same attenuators, must be combined so that A = 32 dB. The azimuth weights could be applied at the column level with P modules. This would increase η_s but complicate the antenna. The relative weightings for the columns and rows were calculated assuming a spacing of $\lambda/2$.[1, 2, 3] Then, the elevation and azimuth modified Bayliss feed network coefficients were obtained from Eq. (1). These separately define the distributions for the center column and row of the antenna and are shown in Figure 12.

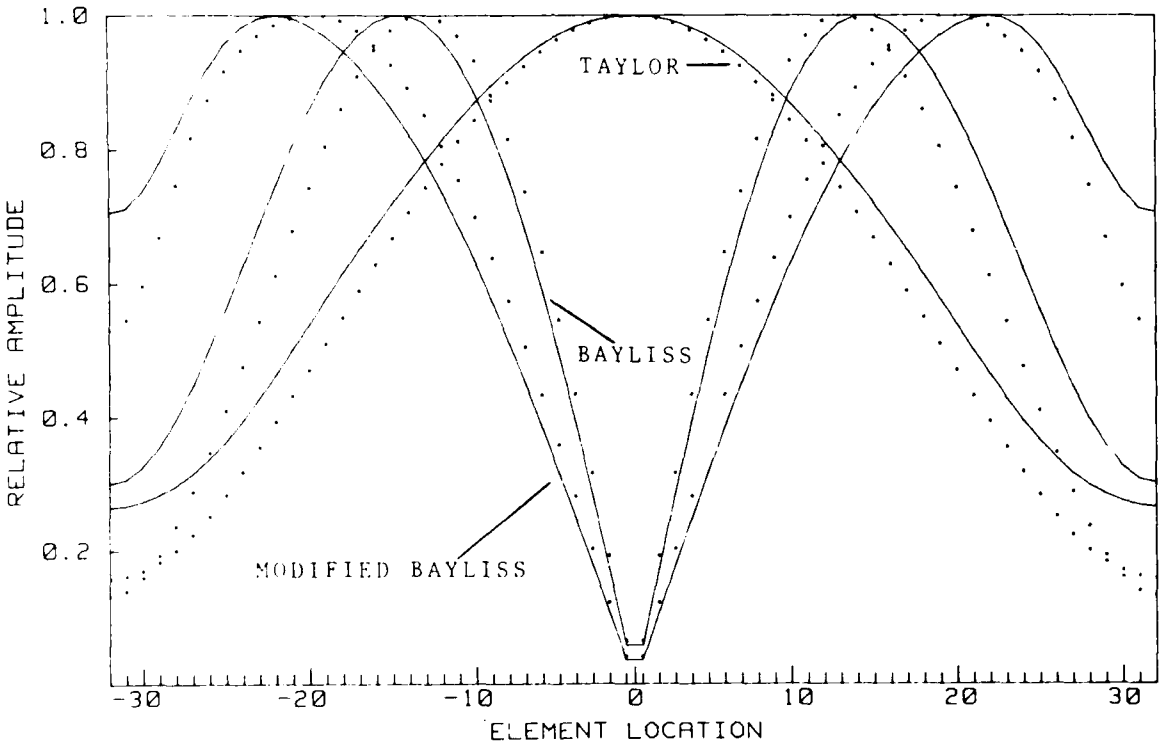

Figure 12. Element Weighting for 64 × 64 Array. Solid curve $\bar{n}$ = 6, SLL = -30 dB and dotted curves $\bar{n}$ = 8, SLL = -40 dB

The taper efficiency from Figure 5 or Eq. (6) is $\eta_t = \eta_{tQ}\,\eta_{tP} = 0.69$. However, the aperture noise suppression efficiency can be similarly factored only if the azimuth weights are applied at the column outputs. Then from Figure 10, $\eta_s = \eta_{sQ}\,\eta_{sP} = 0.99$ and 0.98 for L = -6 dB and -9 dB respectively in each beamformer. When the row and column weights are applied with the same attenuator, Eq. (17) must be rewritten as

$$\eta_s = \sum_{q=1}^{Q}\sum_{p=1}^{P} A_{qp} \Big/ \sum_{q=1}^{Q}\sum_{p=1}^{P} [1 + (1 - A_{qp}L)/A_{qp}LGF] \,. \qquad (18)$$

With F = 3 dB, and G = 30 dB, $\eta_s = 0.96$ and 0.87 for L = -12 dB and -18 dB respectively to account for the losses in both beamformers. Thus applying the total taper at the element level results in an additional loss of about 1/2 dB in S/N ratio. For the same value of G, lower sidelobe levels would result in a greater loss.

To select the number of quantization bits, we assume that the total error consists of four equal parts due to the phase quantization, other phase errors, the amplitude quantization, and other amplitude errors. Furthermore, we require SLL_{rms} to be 6 dB below the SLL. Thus B' is found from Eq. (3) with SLL_{rms} -52 dB. The result is B' = 5 or B' = 7 depending on where the taper is applied.

4. DISCUSSION

A significant reduction in the complexity of the feed network of MMIC active aperture arrays is possible when the modules have internal amplitude control. In this case, one beamformer can be shared between the transmit and the receive sum channel thereby eliminating one of the three feed networks normally required. The T/R switch or circulator that transfers the module input from the transmit to the receive manifold is eliminated as well. It is apparent that in a large array, the total savings in feed network components is formidable.

The calculations have shown that for a range of designs, the component requirements are realistic. For example, LNA gains and noise figures of 30 dB and 3 dB respectively, are adequate and easily achievable. The attenuator requirements, 4 to 6 bits and 20 to 30 dB attenuation range, are also easily implemented with GaAs MMIC technology.

The shared beamformer is applicable to arrays that do not require monopulse processing as well. In this case the two feed networks for each column are

replaced by one. In contrast to this, a sequential lobing (instead of monopulse) array could be implemented with a single beamformer.[7]

There are many other aspects of MMIC antenna integration that must be evaluated before the full potential for this new technology can be realized. Some of these are elimination of the circulator now required to isolate the power amplifier from the scan induced active element impedance variation; improved concepts for energy storage; better solutions for heat removal; techniques for array alignment, calibration, and monitoring; architectures for adaptive nulling; and methods reconfiguration to compensate for failures. As never before, the antenna designer, system analyst, user, and the component developer must work as a team to develop the technology for MMIC active aperture antennas of the future.

---

7. Skolnik, M.I. (1970) The Radar Handbook, McGraw-Hill, New York.

References

1. Hansen, R.C. (1964) Microwave Scanning Antennas, Volume I, Academic Press, New York.
2. Elliot, R.S. (1981) Antenna Theory and Design, Prentice-Hall, Englewood Cliffs, New Jersey.
3. Barton, D.K., and Ward, H.R. (1969) Handbook of Radar Measurement, Prentice-Hall, Englewood Cliffs, New Jersey.
4. Haupt, R.L., Capt. (1982) Simultaneous Nulling in the Sum and Difference Patterns of a Monopulse Antenna, RADC-TR-82-274, AD A131865.
5. Steinburg, B.D. (1976) Principles of Aperture and Array System Design, Wiley, New York.
6. Carlson, B.A. (1975) Communication Systems, 2nd Ed., McGraw-Hill, New York.
7. Skolnik, M.I. (1970) The Radar Handbook, McGraw-Hill, New York.

MISSION
of
Rome Air Development Center

RADC plans and executes research, development, test and selected acquisition programs in support of Command, Control, Communications and Intelligence (C^3I) activities. Technical and engineering support within areas of competence is provided to ESD Program Offices (POs) and other ESD elements to perform effective acquisition of C^3I systems. The areas of technical competence include communications, command and control, battle management, information processing, surveillance sensors, intelligence data collection and handling, solid state sciences, electromagnetics, and propagation, and electronic, maintainability, and compatibility.

Printed by
United States Air Force
Hanscom AFB, Mass. 01731

END

DATE

FILMED

DEC.

1987